Evaluating endogenous repair of focal cartilage defects in C57BL/6 and MRL/MpJ mice using 9.4 T magnetic resonance imaging: A pilot study

J. Mak [a], C. Leonard [a,b], T. Foniok [e], D. Rushforth [e], J.F. Dunn [d,e], R. Krawetz [a,b,c,*]

[a] McCaig Institute for Bone & Joint Health, University of Calgary, Calgary, AB, Canada [b] Department of Surgery, University of Calgary, Calgary, AB, Canada
[c] Department of Anatomy and Cell Biology, University of Calgary, Calgary, AB, Canada [d] Department of Radiology, University of Calgary, Calgary, AB, Canada
[e] Experimental Imaging Centre, University of Calgary, Calgary, AB, Canada

Keywords:

Cartilage
Regeneration
Superhealer
Mouse
MRI

A B S T R A C T

The use of magnetic resonance imaging (MRI) for evaluating joint injuries is often considered superior to radiography due to the capacity of MRI for visualizing both soft and hard tissues. While longitudinal studies regarding cartilage repair have been undertaken on patients and in larger animal models, a method has yet to be developed for mouse cartilage to be repeatedly and non-invasively evaluated over time. The aim of this pilot study was to investigate if morphological changes following a focal cartilage injury in mice could be measured by 9.4 T magnetic resonance imaging. Focal cartilage defects were induced in the left knee of 4–6 weeks old C57BL/6 and MRL/MpJ mice. At endpoints 0, 2, and 4 weeks post-injury, legs were dissected out and imaged *ex vivo*. The defect could be detected by MRI immediately after injury, appearing as a hyperintense focal point and with size similar to that of the surgical tool used. Defects were visible in both strains up to 4 weeks post-injury, although signal intensity decreased over time. One C57BL/6 in particular, displayed extensive fibrosis in the patellar tendon at 4 weeks as assessed by histology, while the MR images of the same animal displayed a clear, structural distinction between the patella and the new tissue growth. Overall, our results suggest that MRI could be used for longitudinal studies in murine cartilage injury models to evaluate certain characteristics of repair not detectable through histology.

1. Background

In most mammals including humans, endogenous cartilage repair is an ineffective process. If the cartilage defect is deep enough to reach the marrow cavity, repair can be observed; however the repair tissue usually consists entirely of fibrocartilage. Fibrocartilage is inferior to hyaline cartilage with respect to robustness since it is composed mainly of collagen type 1 rather than type 2 [1] and is unable to withstand the same mechanical loading as the original hyaline cartilage surface. A number of research groups have independently confirmed the presence of stem cells in the joint environment (synovial membrane and fluid) that are able to differentiate into chondrocytes and produce hyaline like cartilage (*in vitro*), suggesting that an intrinsic cartilage repair mechanism may exist. However, to study cartilage repair *in vivo*, it is necessary to identify appropriate controls that demonstrate some level of endogenous repair. The mouse strain MRL/MpJ (MRL) is of particular interest in this regard. In one study, an intraarticular fracture was induced in C57BL/6 (C57) and MRL mice and evaluated for post-traumatic arthritis [2]. At 4 and 8 weeks after injury, MRL mice did not show the gross morphological changes that occurred in the C57 mice [2]. In a separate study, the authors induced full thickness cartilage lesions in C57 and MRL mice and evaluated injury sites at 6 and 12 weeks [3]. The authors observed that full thickness lesions resulted in significant repair in MRL mice at both 6 and 12 week time points, while limited to no repair was observed in C57 mice over the same period of time [3]. Furthermore, the repair tissue was comprised of chondrocytes and exhibited a hyaline cartilage-like structure including proteoglycan and collagen expression. However, it is important to note that all these studies rely on end point histological examination of the cartilage and this has two important drawbacks; (i) examination of individual animals at different time points does not account for animal to animal variability, and (ii) these methods of cartilage repair assessment cannot be clinically translated.

* Corresponding author at: McCaig Institute for Bone and Joint Health, Faculty of Medicine, University of Calgary, 3330 Hospital Drive NW, Calgary, Alberta, Canada T2N 4N1. Tel.: +1 403 210 6268.
E-mail address: rkrawetz@ucalgary.ca (R. Krawetz).

The use of magnetic resonance imaging (MRI) for cartilage evaluation continues to be intensely evaluated. Compared to the use of X-ray, MRI is ideal due to its capacity to visualize not only cartilage but also the surrounding tissues in the joint. The use of MRI in rodent cartilage repair studies, however, remains limited. Preclinical studies involving focal cartilage repair often utilize large animal models such as rabbits, sheep, dogs, pigs, etc. Murine models are underutilized due to the gross size of the joint, and also the cartilage thickness: rodent cartilage is only a few cells thick and thus correlating mechanisms of degeneration and/or repair in rodents to that of humans is difficult [4]. Despite these potential biological limitations/differences, the wide spectrum of genetic tools that are available in mice makes the use of this animal model ideal to study complex systems and has led to the development of various murine cartilage injury models [2,5]. While longitudinal studies regarding cartilage repair have been undertaken in patients and in larger animal models, a robust method has yet to be developed that will allow for mouse cartilage to be repeatedly and non-invasively evaluated over time.

In this study, we adapted a previously published protocol for mouse model of focal cartilage defect [5] and sought to determine whether MRI could be used to evaluate morphological differences in cartilage repair between C57 and MRL mice.

2. Materials and methods

All animal experiments were done in accordance to the standards of the research ethics committee at the University of Calgary.

2.1. Creating surgical apparatus—stopped needle

A custom made stopped needle was used to induce a standardized cartilage defect. Similar to the needle described by Eltawil et al. [5], a stopper in the form of a bead was made from Apoxie Sculpt® and placed on a 26 gauge (26G) needle (BD Biosciences) such that approximately 1.45 mm of the tip was exposed. For sterilization, stopped needles were exposed to UV radiation for 15 minutes.

2.2. Inducing cartilage defect

The 'pin-prick' technique used in this study for inducing focal cartilage defects has been previously described and validated [5]. Briefly, a small skin incision on the medial side of the left knee was made to expose the patella and the associated tendon. Keeping the knee extended, the tip of our custom-made 26G stopped needle was inserted under the patella tendon from the medial side and aimed towards the femur. Pressure was applied with a rotational motion until the tissue was at the hilt of the stopper. The resistance upon withdrawing the needle and bleeding indicated that the needle had successfully penetrated into the subchondral bone.

2.3. Experimental outline

Focal cartilage defects were induced in the left knee of 4- to 6-week-old mice ($n = 3$ per timepoint, per strain). Injuries were induced in the first group of animals, which were allocated for the $t = 0$ timepoint (euthanized immediately after injury), while remaining animals were euthanized at 1 hour, 2 weeks and 4 weeks post-injury. At the endpoints, both legs were dissected out and fixed with 10% neutral buffered formalin (NBF).

2.4. Magnetic resonance imaging (MRI)

After fixation, samples were imaged *ex vivo* using a 9.4 T/21 cm horizontal bore magnet (Magnex, UK) with a Biospec console (Bruker, Germany) and a cryogenic transceive quadrature RF surface coil (CryoProbe, Bruker, Germany) [6]. A proton density weighted, four-segment Rapid Acquisition with Relaxation Enhancement (RARE) sequence was used with the following parameters: RARE factor = 4, repetition time = 2000 ms, echo time = 9.346 ms, FOV = 1.92 cm, slice thickness = 0.25 mm, matrix = 256 × 256, and averages = 12. Once imaged, samples were processed, embedded into paraffin wax, and sectioned at 7 μm thickness.

2.5. Characterizing defect size by image analysis

Tip to bead distance on the surgical apparatus was measured using calipers. To measure defect size in an MRI scan, pixel size was calculated to be 75 μm × 75 μm with a slice thickness of 250 μm. MRI scan section was saved as a DICOM (.dcm extension) file and subsequently opened with ImageJ software. Under image ➔ properties, unit of length was set to μm, pixel width and depth were set to 75 μm, and voxel depth was set to 250 μm. The defect was measured using the straight line tool, where the length of the drawn line was given. To measure the defect size in the corresponding histological image, the TIF file containing a scale bar was opened with ImageJ. Using the straight line tool, a line was drawn to the length of the scale bar. Under analyze ➔ set scale, length of scale bar and the unit of length was entered into known distance and the box next to 'global selection' was selected. The defect was measured using the straight line tool where length of the line drawn was now presented in the unit of measurement (length) entered. Signal intensity was quantified using SPIN (Magnetic Resonance Imaging Institute for Biomedical Research). The signal intensity of the defect was acquired and then normalized to the signal intensity of the bone marrow in the same mouse. The signal intensity of the defect area was then normalized to the bone marrow signal intensities obtained from each strain of mouse at each time point.

2.6. Histological analysis

Legs were fixed for 3 days in 10% NBF and decalcified in 10% EDTA for three weeks. After decalcification was completed, samples are washed with water and underwent tissue processing and embedding. Paraffin-embedded tissue sections at 7 μm thick were stained with Safranin-O and graded using a scoring matrix previously described [3].

3. Results

3.1. Characterization of the cartilage defect with MRI and histology

Defects induced using 26G needles were characterized using MRI and histology and compared with the measurements of the surgical device itself and non-injured joints (Fig. 1). A representative image of the defect in a disarticulated injured femur (Fig. 1A) has been stained with India ink to demonstrate the position of the defect in the femoral groove. The external diameter of the needle, as provided by the manufacturer (BD Bioscience), was 0.45 mm (450 μm). The length from the tip of the needle to the edge of stopper was approximately 1.45 mm (1450 μm) as measured using calipers. The MRI scans of an injured knee at time 0 post-injury revealed a localized increase in signal intensity below the patella (Fig. 1D, F, H) compared to an MRI of a non-injured leg (Fig. 1B). The hyperintense area was measured using ImageJ and to be 375 μm in diameter and 1125 μm in length for mouse 1 (Fig. 1D), 213 μm by 1025 μm for mouse 2 (Fig. 1F) and 515 μm by 1065 μm for mouse 3 (Fig. 1H). ImageJ analysis of Safranin-O stained sections from the same samples demonstrated a defect opening of 441 μm for mouse 1 (Fig. 1E), 271 μm for mouse 2 (Fig. 1G) and 587 μm for mouse 3 (Fig. 1I).

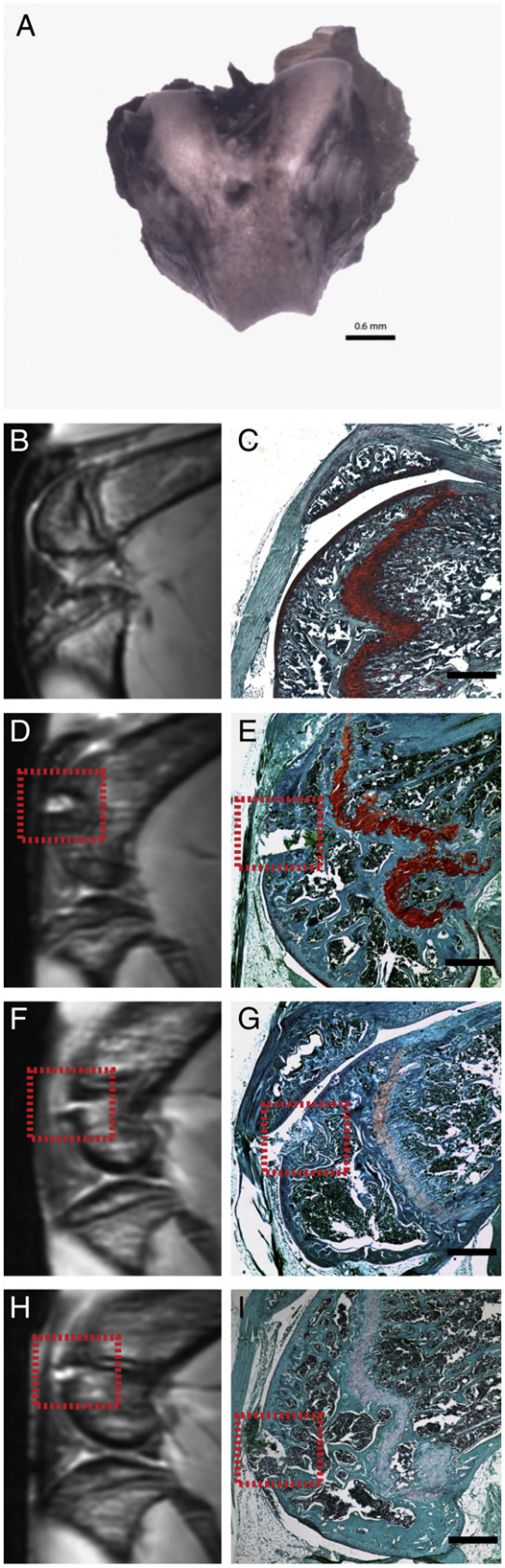

Fig. 1. Visualization of non-injured and injured joints. An isolated mouse femur that has been stained with India ink after injury to demonstrate the relative position of the defect (A). Non-injured knees were assessed using MRI (B) and Safranin-O (C). Injured knees at 0 weeks post-surgery assessed by MRI (D, F, H) and Safranin-O (E, G, I), the defect area is indicated by the yellow boxes. Scale bar equal to 500 μm.

3.2. Defects can be visualized with MRI up to 4 weeks post-injury in both strains

Side by side comparisons of histology and MRI scans show that a focal cartilage injury can be visualized up to 4 weeks in both C57 and MRL mice (Fig. 2). MRI scans for both strains at the 1 hour after injury time point display decreased signal intensity compared to the time 0 images (Fig. 1) within the injury sites, with hyperintense signaling at the defect further decreasing over time in both strains (Fig. 2). Hypointense signaling in the patella and striations were also observed to be localized at load-bearing areas in both MRL and C57 mice (Fig. 2). Compared to non-injured legs, thickness of the hypointense layer at the cartilage surface in C57 mice appeared to decrease after injury (Fig. 2A) but was observed to be maintained in MRL mice (Fig. 2B).

Areas with proteoglycan staining corresponded to areas of hypointense signaling as assessed by MRI (Fig. 2), although the correlation between the two was not exclusive. In some animals, hypointense signaling was present in the corresponding MRI scan in areas where proteoglycan staining in the patellar tendon was not present (Fig. 2). Furthermore, increased signal intensity was observed not only at the site of injury at 1 h after injury, but also at 4 weeks post-defect in two of the three C57 mice that displayed gross morphological changes in the injured knee (Fig. 2A). In these mice hyperintense signaling was observed not only in the defect but also in the tissues surrounding the joint and this was not observed in the MRL mice at 4 weeks (Fig. 2B).

The signal intensity of the defect area was quantified in each strain at each time point and it was found that signal intensity increased after injury in both strains with C57 intensity peaking at 4 weeks (Fig. 2C) and MRL intensity peaking at 2 weeks (Fig. 2D). At 4 weeks post-injury, MRL signal intensity in the defect area had almost returned to control levels, however, C57 levels remained high (Fig. 2E). When the injury was histologically graded a significant difference was also observed between C57 and MRL healing, with MRL mice demonstrating significantly better healing the C57 mice at 4 weeks (Fig. 2F).

4. Discussion

MRI can be used to visualize cartilage in a rodent focal cartilage injury model. Defect size as measured by MRI correlated well with the size of the needle used to make the injury, as well as the defect measurements generated from histological sections. The localized increase in signal intensity at the site of injury is most likely due to an influx in fluid content.

Having established and validated a cartilage injury model, we set out to characterize the early healing process following a focal cartilage injury in both C57 and MRL mice. It was evident that defects could still be visualized for up to 4 weeks post-injury. In both strains, we observed hypointense signaling in the patella and its associated tendon while striations were seen in load bearing areas. These findings have been documented before in humans and have been associated with areas of high collagen and high proteoglycan content [7]. We observed, however, that signal intensity does not always correlate with proteoglycan content. Comparing section histology with the corresponding MRI scan, we also observed that hypointense signaling in the patella and tendon occurs despite low levels of Safranin-O staining.

In support of previous studies [2,3], we found that at 4 weeks post-injury, repair in MRL mice was significantly superior to repair in C57 animals (Fig. 2). Interestingly, two of the C57 animals displayed gross changes in knee morphology at 4 weeks post-injury. Hyperplasia of the patella and the associated tendon was observed but the MRI showed a clear, structural distinction between the patella and

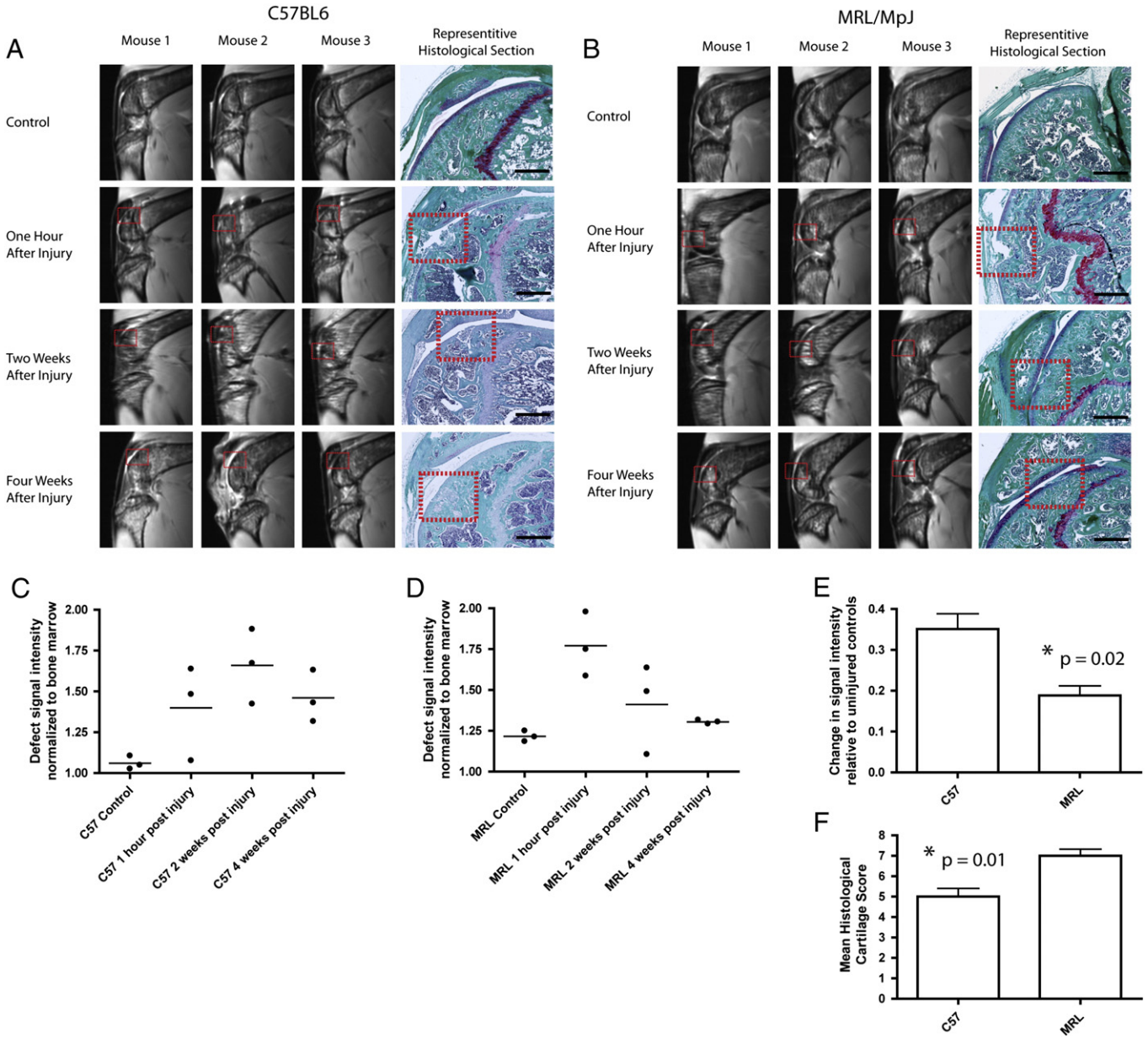

Fig. 2. Histological and MRI analysis of injured knees at 2 and 4 weeks post-injury in both C57BL/6 (A) and MRL/MpJ (B) mice. Quantification of signal intensity in the defect area of C57 (C) and MRL (D) demonstrates that MRL mice have a lower signal intensity at 4 weeks post-injury compared to C57 mice at the same time point (E). This corresponds with MRL mice demonstrating a significantly better repair compared to C57 mice (F). Defects are highlighted in the red boxes in both the Safranin-O stains as well as in the respective MRI scans. Scale bar equal to 500 μm.

the new tissue growth (Fig. 2). The latter is associated with an increase in signal intensity while the patella is clearly outlined by the hypointense signaling. Hyperintensities could be due to changes in water content but this seems unlikely to be the sole reason due to the fibrotic appearance of the new growth. A more plausible cause could be due to changes in collagen fibers and other structural components that resulted in the increase in signal intensity [8,9].

Nevertheless, our data suggest that *ex vivo* MRI can reveal structural and morphological changes in the joint tissue in response to injury that is not evident in histology. Further analysis to distinguish how signal intensity corresponds to the composition of repair tissue will be needed before MRI can be used as a tool for monitoring *in vivo* mouse models of cartilage injury.

Acknowledgments

The study was supported by the Canadian Stem Cell Network, Natural Sciences and Engineering Research Council of Canada and Canadian Institutes of Health Research.

References

[1] Gerter R, Kruegel J, Miosge N. New insights into cartilage repair—the role of migratory progenitor cells in osteoarthritis. Matrix Biol 2012;31:1–8.
[2] Ward BD, Furman BD, Huebner JL, Kraus VB, Guilak F, Olson SA. Absence of posttraumatic arthritis following intraarticular fracture in the MRL/MpJ mouse. Arthritis Rheum 2008;58:744–53.
[3] Fitzgerald J, Rich C, Burkhardt D, Allen J, Herzka AS, Little CB. Evidence for articular cartilage regeneration in MRL/MpJ mice. Osteoarthritis Cartilage 2008;16:1319–26.

[4] Ahern BJ, Parvizi J, Boston R, Schaer TP. Preclinical animal models in single site cartilage defect testing: a systematic review. Osteoarthritis Cartilage 2009;17:705–13.
[5] Eltawil NM, De Bari C, Achan P, Pitzalis C, Dell'accio F. A novel in vivo murine model of cartilage regeneration. Age and strain-dependent outcome after joint surface injury. Osteoarthritis Cartilage 2009;17:695–704.
[6] Wagenhaus B, Pohlmann A, Dieringer MA, Els A, Waiczies H, Waiczies S, et al. Functional and morphological cardiac magnetic resonance imaging of mice using a cryogenic quadrature radiofrequency coil. PLoS One 2012;7:e42383.
[7] Foster JE, Maciewicz RA, Taberner J, Dieppe PA, Freemont AJ, Keen MC, et al. Structural periodicity in human articular cartilage: comparison between magnetic resonance imaging and histological findings. Osteoarthritis Cartilage 1999;7:480–5.
[8] Shimono T, Akai F, Yamamoto A, Kanagaki M, Fushimi Y, Maeda M, et al. Different signal intensities between intra- and extracranial components in jugular foramen meningioma: an enigma. AJNR Am J Neuroradiol 2005;26:1122–7.
[9] Goodwin DW, Wadghiri YZ, Dunn JF, Density P, Effect A. Micro-imaging of articular cartilage: T2, proton density, and the magic angle effect. Acad Radiol 1998;5:790–8.